

Article

# Study on the Performance of Photovoltaic/Thermal Collector–Heat Pump–Absorption Chiller Tri-Generation Supply System

Han Yue <sup>1</sup>, Zipeng Xu <sup>1</sup>, Shangling Chu <sup>1</sup>, Chao Cheng <sup>2,\*</sup>, Heng Zhang <sup>1,3</sup> , Haiping Chen <sup>1,3</sup> and Dengxin Ai <sup>4</sup>

<sup>1</sup> School of Energy, Power and Mechanical Engineering, North China Electric Power University, Beijing 102206, China

<sup>2</sup> National Institute of Energy Development Strategy, North China Electric Power University, Beijing 102206, China

<sup>3</sup> Beijing Key Laboratory of Pollutant Monitoring and Control in Thermolectric Production Process, North China Electric Power University, Beijing 102206, China

<sup>4</sup> State Grid Tianjin Electric Power Company, Tianjin 300232, China

\* Correspondence: chengc@ncepu.edu.cn

**Abstract:** The solar energy supply system has played an increasingly substantial role in realizing nearly zero-carbon buildings. In order to overcome the impact of solar randomness on the energy supply of a distributed solar system, this paper proposes a solar tri-generation supply system which integrates a photovoltaic/thermal collector (PV/T), a heat pump (HP), and an absorption chiller (AC). The PV/T-HP integration system is adopted to provide stable heating for a building and AC. The system model is established in TRNSYS software, and its performance is evaluated based on energy, exergy, and economic aspects. The results demonstrate that the system effectively meets the load demand, with an energy efficiency of 32.98% and an exergy efficiency of 17.62%. The payback period (PP) is 7.77 years. Compared with the systems proposed in the other literature, the performance of the proposed system has a certain extent of advantage. Furthermore, the equipment and system exergy performance decline with an increase in the intensity of solar radiation. Increasing the PV/T area effectively improves the system's profitability within the actual roof area limitation of the building. Moreover, increasing the capacity of the low-temperature heat pump after 68 kW improves the system efficiency and reduces the payback period. In summary, this paper proposes an efficient distributed solar energy system that is suitable for urban building energy supply.

**Keywords:** photovoltaic/thermal; water source heat pump; solar tri-generation; transient simulation; multi-criteria analysis



**Citation:** Yue, H.; Xu, Z.; Chu, S.; Cheng, C.; Zhang, H.; Chen, H.; Ai, D. Study on the Performance of Photovoltaic/Thermal Collector–Heat Pump–Absorption Chiller Tri-Generation Supply System. *Energies* **2023**, *16*, 3034. <https://doi.org/10.3390/en16073034>

Academic Editors: Adam Idzkowski, Maciej Zajkowski, Zbigniew Sołjan and Stanislav Darula

Received: 27 February 2023

Revised: 21 March 2023

Accepted: 22 March 2023

Published: 27 March 2023



**Copyright:** © 2023 by the authors. Licensee MDPI, Basel, Switzerland. This article is an open access article distributed under the terms and conditions of the Creative Commons Attribution (CC BY) license (<https://creativecommons.org/licenses/by/4.0/>).

## 1. Introduction

### 1.1. Motivation and Incitement

Carbon emissions from a building's energy supply may be significantly reduced by cutting down on fossil fuel usage and increasing the use of renewable energy sources. Residential buildings generate 22 percent of global energy consumption and 17 percent of carbon emissions [1]. Integrating renewable energy and buildings is crucial to decarbonizing the building sector. The Chinese government has proposed a technical standard of buildings with near-zero energy consumption which defines zero-carbon buildings as those with a renewable energy output equal to or greater than their energy consumption [2]. The renewable energy with the greatest potential to decarbonize the building in such a situation is solar energy [3]. In addition, the installed capacity of PVs has increased rapidly in the past decade, and it is higher than other renewable energy technologies [4].

Currently, researchers are conducting studies to improve the efficiency of photovoltaic (PV) cells [5,6]. However, due to the material limitations of crystalline silicon, a commercial

photovoltaic (PV) cell only has an efficiency of 21% in converting solar energy [7]. Therefore, increasing the effectiveness of solar energy use is the most important challenge when facing solar energy technology. The photoelectric conversion efficiency of a PV cell will decline as its surface temperature rises [8]. The maximum working temperature of a standard PV cell is 110 °C, and the efficiency reduces 0.452% for every 1 °C rise in surface temperature after it reaches 25 °C [9]. In recent years, to mitigate the temperature effect on the performance of a PV cell, the integration of the PV cell and a collector, known as a photovoltaic/thermal collector (PV/T), has been proposed by many researchers. This integration has led to a higher solar energy utilization efficiency due to the cooling effect of the PV/T [10,11]. In short, compared with a PV cell and solar collector, the PV/T has good application potential in urban areas with a limited roof area [11].

In addition to solar energy technology, a heat pump (HP) is also considered the most promising technology that adopts renewable energy to provide space heating and cooling for residential buildings [12]. A heat pump provides heat energy at a higher temperature by using a low-temperature energy source, such as air, geothermal and water sources. A water source heat pump has a higher coefficient of performance (COP) compared to an air source heat pump [13]. In addition, a heat pump can be also combined well with solar energy technology to provide heat [14]. Many studies focus on the coupling of solar collectors and heat pumps, while PV/T can generate both electricity and heat. Therefore, the integration of a PV/T and a heat pump has greater advantages than a traditional solar collector coupled with a heat pump [15]. In the context of urban building heating, the integration of a water-based PV/T and a water source heat pump is considered to be more efficient and reliable compared to the integration of an air-based PV/T and an air source heat pump [16].

In summer, however, the combination of a PV/T and a water source HP system cannot fulfill the cooling demand of building [17]. Absorption chillers (ACs), which are heat-driven cooling devices, are attractive due to the low-temperature heat source requirement [18]. Therefore, the utilization of solar energy technology could be a potential option for integration with absorption chillers, making solar-absorption chiller integration a promising option [19].

In general, many studies have designed an absorption chiller to achieve the balance between a PV/T's hot water output and an absorption chiller's heat source by reducing the heat source temperature demand. However, compared with a solar collector coupled with an absorption chiller, a hot water PV/T can only meet the temperature requirement of an absorption chiller for a shorter duration of time due to the inability of the PV cell to withstand a high operating temperature, which is highly disadvantageous for cooling an urban building [20]. Moreover, previous studies have mainly focused on the performance analysis of a PV/T and absorption chiller integration system; therefore, the impacts of the randomness of solar energy and the variability of the building load are barely considered, posing significant challenges to the reliability of the integration system.

### *1.2. Literature Review and Research Gap*

Many scholars conducted extensive research on PV/Ts which focused on optimizing the structure of the PV/T to achieve better electric and thermal performance. Kazem et al. compared a PV and a PV/T and found that the PV/T had a 6% higher power output than the PV [21]. Typically, the common cooling fluids in a PV/T are mainly divided into water and air, with water-based PV/Ts having a higher efficiency due to the better heat transfer performance of water [22]. Odeh et al. conducted an experimental study on a heat-pipe-based PV/T for residential use. The results showed that the overall efficiency varied between 26% and 65% at the outlet temperature of 30 °C during the winter, and the PV/T had a payback period of 5–6 years [23]. Maoulida et al. investigated the operational performance of a PV/T using TRNSYS. A PV/T in the Koua region met 70% of the annual hot water demand and 80% of the electricity demand, demonstrating a maximum efficiency of 40% [24]. Hassan et al. investigated the influence of different parameters on

the performance of a water-based PV/T, and their results showed that the average thermal efficiency, electrical efficiency, and overall efficiency of the PV/T were 10%, 20%, and 30%, respectively. Increasing the collector tube diameter and Reynolds number effectively reduced the cell temperature and improved the heat transfer performance of a PV/T [25]. Kalateh et al. proposed the energy, exergy, and entropy analysis of a water-based PV/T with clockwise and counter-clockwise twisted tapes: the electric efficiency and thermal efficiency of the PV/T were 12.51% and 67.49%, respectively, while the electric exergy efficiency and thermal exergy efficiency were 12.76% and 2.10%, respectively. The twisted tapes were able to reduce the entropy increase of the PV/T [26]. Parthiban et al. developed a three-dimension thermal model of a PV/T and studied the influence of environmental and input parameters on the PV/T was studied. A techno-economic analysis was also conducted. The annual energy cost of the PV/T was 0.13 USD/kWh [27]. Gao et al. established a low-concentration PV/T (LCPV/T) model, and the energy efficiency and exergy efficiency of the LCPV/T were analyzed under different environmental conditions. The result showed that the electrical performance and thermal performance of the LCPV/T were significantly affected as the environmental temperature, wind speed, and solar irradiance changed [28]. In general, the effectiveness, economic advantages, safety, and dependability of PV/Ts have all been supported by multiple research studies [7]. In short, compared with traditional PVs and solar collectors, the PV/T has good application potential in urban areas with a limited roof area [29]. However, it is undeniable that PV/Ts are still unable to independently eliminate the impacts of environmental factors. Therefore, PV/Ts need to be matched with an auxiliary energy supply device to achieve a stable energy supply.

Numerous studies focus on the coupling of a solar collector and heat pump, while a PV/T generates both electricity and heat. Therefore, the integration of a PV/T and a heat pump has greater advantages than the coupling of a traditional solar collector with a heat pump [30]. Pakere et al. conducted a multi-criteria assessment for a solar power plant and found that using a heat pump to convert excess electricity into practical thermal energy improved the facility's performance [31]. In fact, a heat pump can assist the PV/T in space heating due to the similar heat output quality between the PV/T and the heat pump [32]. Mi et al. designed a PV/T-HP system in which a PV/T was adopted as the heat pump's cold side; its power generation compensated for the power consumption of heat pump, which was only 32% of the heat pump's consumption when it was operated alone [33]. Bae et al. investigated the annual performance of a PV/T and air source heat pump integrated system in which the PV/T was arranged in parallel with the air source heat pump. The results showed that the electricity generated by the PV/T met the system energy consumption. The COP was 16.3 when in cooling mode and 5.3 in heating mode [34]. Yao et al. performed an experimental study on a newly developed PV/thermal hybrid module that integrated an air source HP. The suggested system had a coefficient of performance (COP) that was 42.9% more than the HP alone [35]. Rijvers et al. established a PV/T and heat pump system model in TRNSYS in which the PV/T was directly connected to the evaporator of the heat pump. Energy and economic analyses were conducted, and the impact of different PV/T areas and types in the system was researched [36]. Kong suggested a PV/T-HP system and investigated the energy and economic assessments, demonstrating that the interaction of the PV/T and HP can improve performance [37]. To enhance energy use efficiency, it is desirable to investigate a PV/T combined with a heat pump. Therefore, the application potential of PV/T-HP systems for building energy supply is substantial.

Research on solar energy and absorption refrigeration mainly focuses on reducing the heat source temperature of the absorption chiller, which is generally achieved through reform to the absorption chiller or by adopting a less energy-efficient absorption chiller. Li et al. developed a solar-absorption cooling hybrid system using subcooled compression, realizing that by lowering the heat source temperature demand of the absorption chiller by 60 °C, the low-grade heat energy of the PV/T could be fully utilized [38]. Aneli et al. investigated a PV/T-AC system model and made a comparison with a conventional vapor compressor chiller (VCC) driven by a PV cell. The PV/T combined with an absorption

chiller showed great performance in net power generation and cooling [18]. Chen et al. proposed a PV/T combined cooling, heating and power (CCHP) system. The results indicated that hot water met the temperature demand of the half-effect absorption chiller (60 °C), and the solar performance coefficient was 0.072 [39].

Based on the literature summarized above, it can be concluded that the key factor in the integration system is that a PV/T can provide stable heat to an absorption chiller. While there have been many studies on the coupling of PV/Ts and absorption chillers, few of them have considered the challenge that solar energy fluctuations may have a negative impact on the system stability in building cooling applications. A PV/T coupled with a heat pump system can provide stable heating, but there still has been no research conducted to verify the potential when a PV/T and heat pump are adopted to provide heat to an absorption chiller.

### 1.3. Contributions and Paper Organization

The main innovation and contribution of this study is the adoption of a PV/T-HP (HP) system to solve the problem of temperature mismatch and unstable heat supply in a PV/T-AC coupling system. A PV/T-HP-AC tri-generation system is proposed that is suitable for urban buildings with the aim of achieving efficient energy management and improving economic viability for a distributed solar energy system.

In this study, a transient simulation model of the PV/T-HP-AC system is constructed using TRNSYS. Energy, exergy, and an economic analysis are investigated in a performance evaluation. In addition, three key parameters, the solar radiation intensity, PV/T area, and the rated capacity of a low-temperature heat pump (LHP), are selected for parametric analysis, which provides a foundation for the further improvement of system performance and optimization.

The rest of this work is organized as follows. Section 2 introduces the system structure and control strategy. Section 3 establishes the thermodynamic model and presents the system evaluation indicators. Section 4 provides validation for the component model in the proposed system. Section 5 proposes a simulation analysis. Finally, Section 6 concludes this paper.

## 2. System Description

A schematic representation of the solar tri-generation supply system is displayed in Figure 1. The system comprises a photovoltaic/thermal collector (PV/T), low-temperature water-to-water heat pump (LHP), high-temperature water-to-water heat pump (HHP), absorption chiller (AC), and thermal storage tank (TES). The HHP is used for producing higher-temperature water for the absorption chiller, while the LHP is adopted to supply space-heating water. The AC is a lithium bromide/water (LiBr/H<sub>2</sub>O) single-effect absorption chiller. The system energy requirement is first met by power production from the PV/T power, after which the TES stores hot water from the PV/T. During the summer, hot water in the TES is adopted as a heat source for the HHP, and the heat source of the AC is provided by the HHP. In the winter, when the outlet temperature of the TES cannot meet the space heating requirement, the hot water is used as a heat source for the LHP, and the heating load is met by the LHP. The model and the corresponding analysis are established in TRNSYS software, and all components adopted in this system are provided by the TRNSYS component library. The components and parameters used in the system are shown in Table 1.

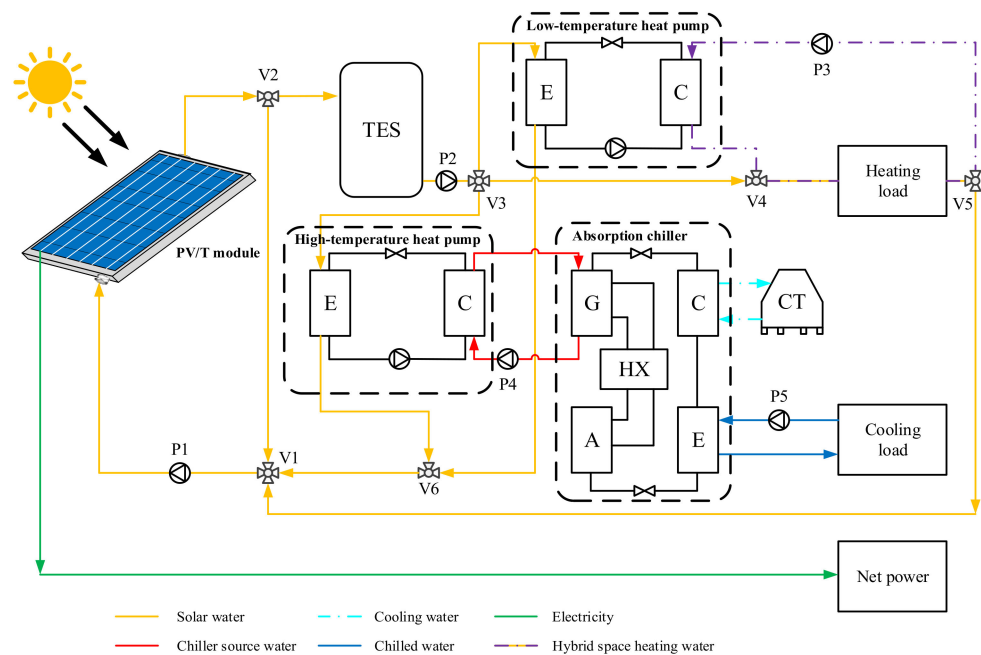


Figure 1. Schematic representation of solar tri-generation supply system.

Table 1. The components and parameters of the system.

Parameter	Value
PV/T (Type 50b)	
Collector area	500 m <sup>2</sup>
Collector fin efficiency factor	0.96
Absorptance of collector plate	0.92
Emittance of collector plate	0.09
Bottom and edge losses coefficient	1.1 kJ/(h·m <sup>2</sup> ·K)
Collector slope	38°
Temperature coefficient of PV cell	0.0032 K <sup>-1</sup>
Nominal Temperature for cell	25 °C
Nominal cell efficiency	21%
Low-temperature heat pump (Type 927)	
Rated heating capacity	15 kW
Rated heating power	3 kW
Number of identical heat pumps	4
High-temperature heat pump (Type 927)	
Rated heating capacity	10 kW
Rated heating power	3 kW
Number of identical heat pumps	10
Absorption chiller (Type 107)	
Rated capacity	65 kW
Rated C.O.P.	0.6
Auxiliary power	0.5 kW
Thermal storage tank (Type 39)	
Overall tank volume	20 m <sup>3</sup>
Tank circumference	1.5 m
Cross section area	4.0 m <sup>2</sup>
Average loss coefficient	5.0 kJ/(h·m <sup>2</sup> ·K)

The functioning of the equipment is mostly influenced by the monitoring of the dormitory's indoor temperature. In order to keep the indoor temperature within the range that the human body finds acceptable, the system is switched to heating mode when the temperature inside is below 18 °C and to cooling mode when it exceeds 28 °C. When the outlet temperature of the PV/T is under 30 °C, V2 is controlled to make water flow back to the PV/T through V1 for self-circulation heating. All the generated hot water is collected in the TES and is applied for directly space heating or as the auxiliary heat source of other equipment, according to the parameters of the TES. In heating mode: (1) direct heating supply mode: if the outlet temperature of the TES reaches 40 °C, hot water is directly used for heating by controlling V3. (2) Auxiliary heating mode: if the outlet temperature of the TES is under 40 °C, V3 is set by controller to guide the water to the evaporator of the LHP with the operation of the LHP, and the hot water heated by LHP flows from the condenser for the building. Moreover, the HHP is introduced, and the PV/T outlet water is adopted as the HHP's heat source to improve performance.

### 3. System Model

#### 3.1. Building Model

A typical student dormitory located in Tianjin, which is shown as Figure 2, was established as building model to assess the energy supply by system. Tables 2 and 3 show the parameters of the dormitory, which was designed according to the regional building standard. Furthermore, the meteorological data of Tianjin was considered the input for the building model. Figure 3 presents the meteorological data of a typical year in Tianjin. Figure 4 shows the radiation intensity in Tianjin; the maximum radiation intensity is 940 W/m<sup>2</sup>. Figure 4 shows that the average radiation intensity is small due to the cloudy and rainy weather in summer. The heating load of the dormitory model is shown in Figure 5. When the load type is a heating load, the output value is negative, and the value of the cooling load is positive. The maximum heating load is 84.6 kW. Figure 6 shows the annual cooling load. The maximum cooling load is 71.4 kW.

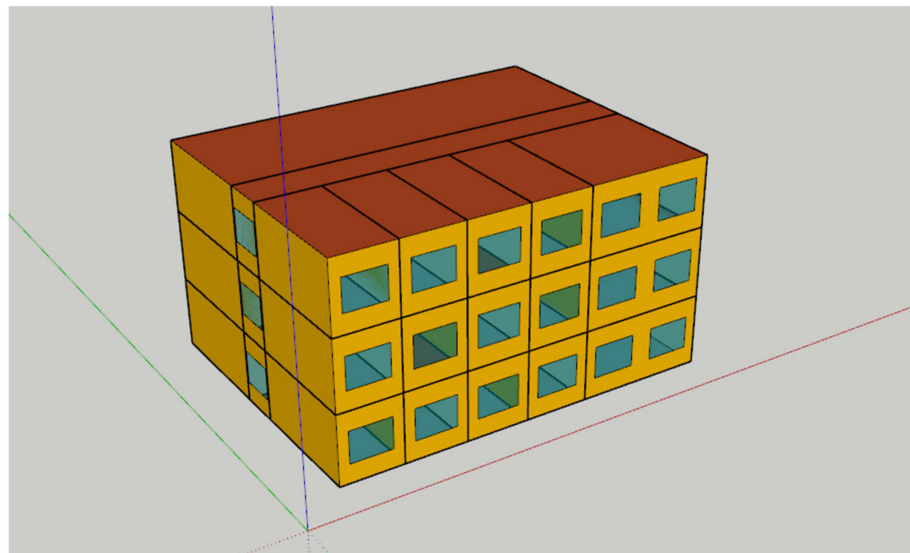


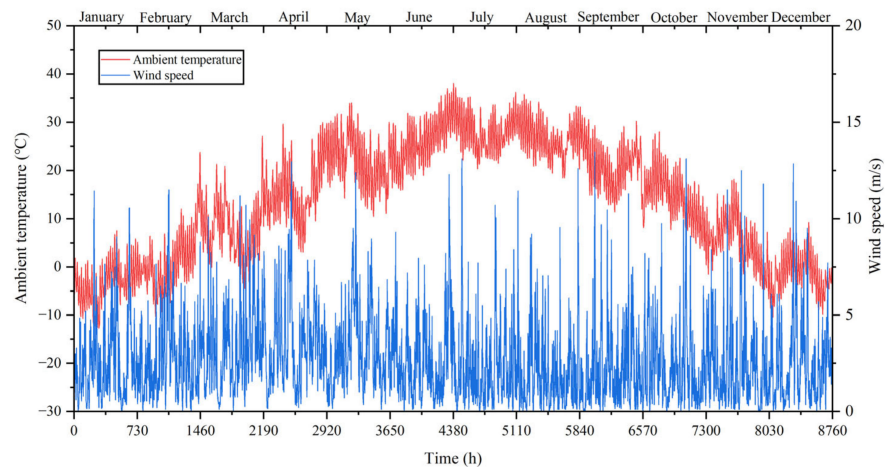
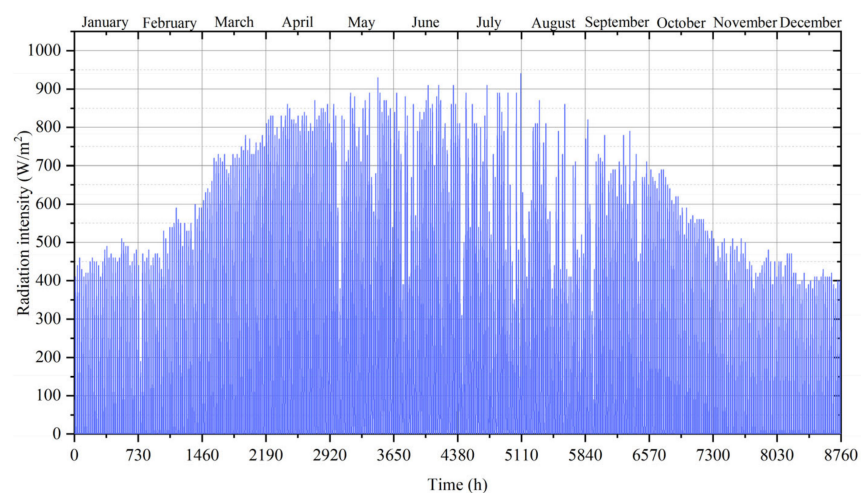
Figure 2. External structure of dormitory model.

**Table 2.** Structural parameter of dormitory model.

Parameter	Value	Unit
Overall area	2142	m <sup>2</sup>
Floor	3	-
Living room area	18	m <sup>2</sup>
Room height	3.3	m
South window–wall ratio	30.30	%
North window–wall ratio	30.30	%
West window–wall ratio	4.33	%
East window–wall ratio	4.33	%
Rated power of computer	320	W
Number of computers in each room	4	-

**Table 3.** Heat transfer coefficient of wall.

Parameter	Value	Unit
External wall	0.349	W/(m <sup>2</sup> ·K)
Internal wall	1.531	W/(m <sup>2</sup> ·K)
Floor	0.663	W/(m <sup>2</sup> ·K)
Ceiling	0.896	W/(m <sup>2</sup> ·K)
Roof	0.304	W/(m <sup>2</sup> ·K)
Window	1.08	W/(m <sup>2</sup> ·K)

**Figure 3.** Hourly ambient temperature and wind speed in Tianjin, China.**Figure 4.** Hourly radiation intensity in Tianjin, China.

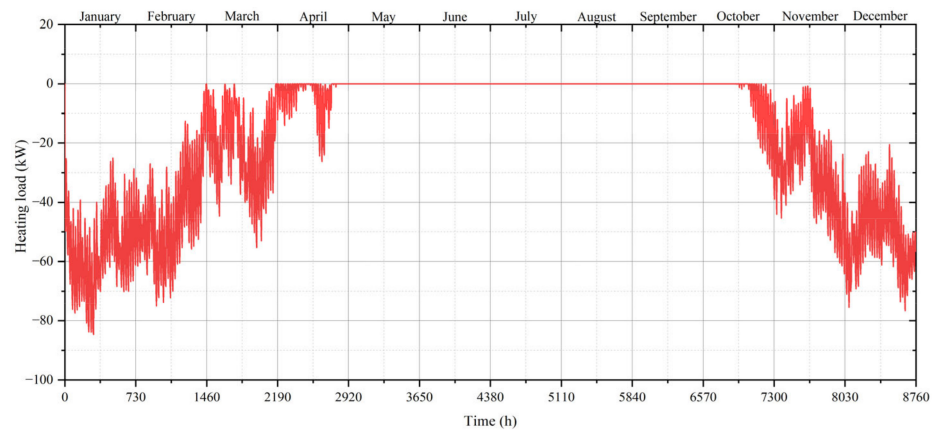


**Figure 5.** Hourly heating load of dormitory.

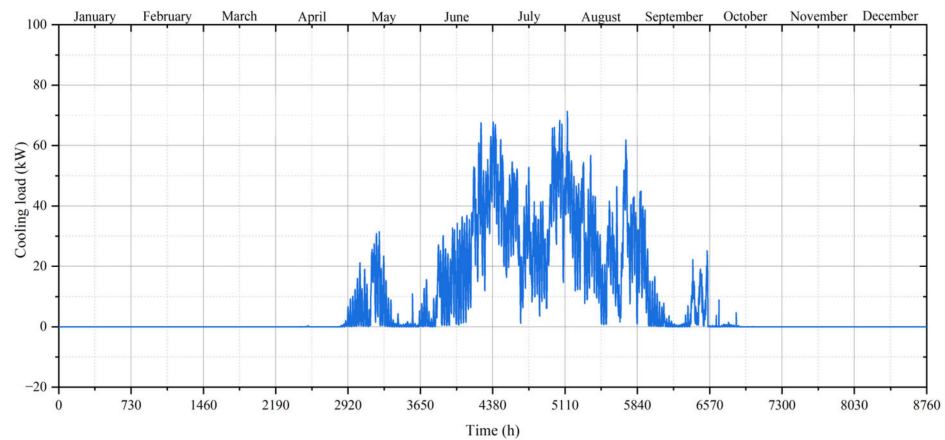


**Figure 6.** Hourly cooling load of dormitory.

### 3.2. Modeling and Analysis

This part describes the mathematical model of system. In the simulation process, the time step of TRNSYS was set to one hour. In the model procedure, the following assumptions were considered [40]:

- The boiling or condensation of working fluid was not regarded;
- The energy loss and fluid leakage caused by the pipe and valve between the equipment connection are considered negligible;
- Potential energy and a change in kinetic energy are ignored.

#### 3.2.1. Balance of Energy and Exergy

The following is the balancing equation for energy and exergy [41]:

$$\dot{E}n_{l,k} = \dot{E}n_{f,k} - \dot{E}n_{p,k} \quad (1)$$

where  $\dot{E}n_{l,k}$  is the  $k$ th component's energy loss;  $\dot{E}n_{f,k}$  is the  $k$ th component's fuel energy;  $\dot{E}n_{p,k}$  is the  $k$ th component's product energy.

$$\dot{E}x_{l,k} = \dot{E}x_{f,k} - \dot{E}x_{p,k} \quad (2)$$

where  $\dot{E}x_{l,k}$  is the  $k$ th component's exergy loss;  $\dot{E}x_{f,k}$  is the  $k$ th component's fuel exergy;  $\dot{E}x_{p,k}$  is the  $k$ th component's product exergy.

### 3.2.2. PV/T Analysis

The electrical and thermal efficiency of the PV/T are as follows [42]:

$$\eta_{el} = \frac{P}{\tau_g G A_{pv}} \quad (3)$$

$$\eta_{th} = \frac{\dot{Q}}{\dot{E}n_{solar,in}} = \frac{\dot{Q}}{\tau_g G A_{pv}} \quad (4)$$

$$\dot{Q} = c_p \dot{m} (T_{out} - T_{in}) \quad (5)$$

where  $\eta_{el}$  (%) is the electrical efficiency of the PV cell,  $G$  ( $W/m^2$ ) indicates the received solar radiation intensity,  $P$  (W) is the electrical power of the PV/T,  $\tau_g$  is the glass cover plate transmittance,  $c_p$  ( $J/(kg \cdot K)$ ) is the specific heat capacity,  $\dot{m}$  ( $kg/s$ ) is the mass flow rate,  $T_{out}$  and  $T_{in}$  (K) are the outlet and inlet temperature.

The overall energy efficiency is calculated by:

$$\eta_{PV/T} = \eta_{el} + \eta_{th} \quad (6)$$

First, the solar exergy obtained by the PV/T is calculated as [43]:

$$\dot{E}x_{in} = \dot{E}x_{solar,in} = \dot{E}n_{solar,in} \psi_s \quad (7)$$

where  $\psi_s$  is the conversion coefficient of solar radiation exergy, and  $\psi_s$  is defined as:

$$\psi_s = 1 - \frac{4}{3} \cdot \frac{T_0}{T_{sun}} + \frac{1}{3} \cdot \left( \frac{T_0}{T_{sun}} \right)^4 \quad (8)$$

where  $T_0$  (K) is the reference temperature (dead state),  $T_{sun}$  (K) is the sun surface temperature ( $T_{sun} = 6000$  K).

Therefore, the PV/T's electrical and thermal exergy efficiency are as follows:

$$\zeta_{el} = \frac{\dot{E}x_{el}}{\dot{E}x_{solar,in}} = \frac{P}{\psi_s G A_{pv}} = \frac{\eta_{el} G A_{pv}}{\psi_s G A_{pv}} = \frac{\eta_{el}}{\psi_s} \quad (9)$$

$$\zeta_{th} = \frac{\dot{E}x_{th}}{\dot{E}x_{solar,in}} = \frac{\dot{m} c_p [(T_{out} - T_{in}) - T_a \ln \frac{T_{out}}{T_{in}}]}{\psi_s G A_{PV}} \quad (10)$$

where  $\dot{E}x_{el}$  (W) is the electric exergy rate and  $\dot{E}x_{th}$  (W) the is thermal exergy rate.

### 3.2.3. Heat Pump Analysis

The heat absorption of the evaporator is as follows [44]:

$$\dot{Q}_E = \dot{m}_E c_p (T_{E,in} - T_{E,out}) \quad (11)$$

where  $\dot{m}_E$  ( $kg/s$ ) is the evaporator's mass flow rate and  $T_{E,in}$  and  $T_{E,out}$  (K) represent the evaporator's inlet and outlet temperatures.

Similarly, when referring to condensers, the heat rate is defined as:

$$\dot{Q}_C = \dot{m}_C c_p (T_{C,out} - T_{C,in}) \quad (12)$$

where  $T_{C,in}$  and  $T_{C,out}$  (K) are the condenser's inlet and outlet temperature and  $\dot{m}_C$  ( $kg/s$ ) is the condenser's mass flow rate.

In general, the COP is shown as:

$$COP_{HP} = \frac{\dot{Q}_C}{\dot{W}_{HP}} = \frac{\dot{Q}_C}{\dot{Q}_C - \dot{Q}_E} \quad (13)$$

where  $\dot{W}_{HP}$  (W) is the power consumption of the heat pump.

The exergy destruction is a significance indicator, and the exergy balance of the heat pump is defined as:

$$\dot{E}x_E + \dot{W}_{HP} = \dot{E}x_C + \dot{E}x_{d,HP} \quad (14)$$

where  $\dot{E}x_E$  and  $\dot{E}x_C$  (W) are the exergy rate of the evaporator and condenser and  $\dot{E}x_{d,HP}$  (W) is the exergy destruction of the heat pump.

The exergy rate of the evaporator and condenser are calculated by:

$$\dot{E}x_E = \left(1 - \frac{T_0}{T_E}\right) \dot{Q}_E \quad (15)$$

$$\dot{E}x_C = \left(1 - \frac{T_0}{T_C}\right) \dot{Q}_C \quad (16)$$

where  $\overline{T}_E$  (K) represents the evaporator's average temperature and  $\overline{T}_C$  (K) is the condenser's average temperature.

In summary, the exergy efficiency is expressed as:

$$\zeta_{HP} = \frac{\dot{E}x_C - \dot{E}x_E}{\dot{W}_{HP}} \quad (17)$$

#### 3.2.4. Absorption Chiller Analysis

Since the absorption chiller's heat source comes from heat of the HHP's condenser, it is defined as [45]:

$$\dot{Q}_G = c_p \dot{m}_G (T_{G,in} - T_{G,out}) \quad (18)$$

where  $\dot{Q}_G$  (kW) is the thermal power of the generator,  $\dot{m}_G$  (kg/s) is the mass flow of the generator, and  $T_{G,in}$  and  $T_{G,out}$  (K) are the inlet and outlet temperatures of the generator.

The cooling capacity of the chilled water from the absorption chiller is shown as:

$$\dot{Q}_E = c_p \dot{m}_E (T_{E,out} - T_{E,in}) \quad (19)$$

where  $\dot{Q}_E$  (kW) is the refrigerating capacity of the evaporator,  $T_{E,in}$  and  $T_{E,out}$  (K) are the inlet and outlet temperatures of the evaporator, and  $\dot{m}_E$  (kg/s) is the mass flow of the evaporator.

The following formula shows the calculations of the COP and exergy efficiency [46]:

$$COP_{ac} = \frac{\dot{Q}_E}{\dot{Q}_G + \dot{W}_{ac}} \quad (20)$$

$$\zeta_{ac} = \frac{-\dot{Q}_E \left(1 - \frac{T_0}{T_E}\right)}{\dot{Q}_G \left(1 - \frac{T_0}{T_G}\right) + \dot{W}_{ac}} \quad (21)$$

where  $\overline{T}_E$  (K) is the average temperature and  $\overline{T}_G$  (K) is the average temperature.

### 3.2.5. Connection Component Analysis

In addition to the exergy change of the equipment, it is essential to consider the data of a state point in the other part in the system. The calculation method for the specific exergy value is introduced, as shown below [47]:

$$\begin{aligned} ex_{ph} &= (h - h_a) - T_a(s - s_a) \\ &= c[(T - T_a) + v(p - p_a)] - T_a c \ln\left(\frac{T}{T_a}\right) \end{aligned} \quad (22)$$

where  $ex_{ph}$  is the specific physical exergy,  $h$  is the specific enthalpy of the state point,  $s$  is the specific entropy,  $p$  is the pressure, and the subscript  $a$  indicates the ambient parameter. It should be noted that no chemistry process occurs, and no phase change process happens during operation; therefore, the equation can be simplified as follows:

$$ex_{ph} = c_p(T - T_a) - T_a c_p \ln\left(\frac{T}{T_a}\right) \quad (23)$$

### 3.2.6. System Comprehensive Evaluation Indicator

The evaluation indicators of the system include the energy efficiency, exergy efficiency and payback period. The system energy efficiency is shown below [48]:

$$\eta_{sys} = \frac{P + \dot{Q}_h + \dot{Q}_c}{\dot{W}_{con} + \dot{E}n_{solar,in}} \quad (24)$$

where  $\dot{Q}_h$  and  $\dot{Q}_c$  (W) are the output energy of the hot water and chilled water and  $\dot{W}_{con}$  (W) is the electricity consumption of system.

The exergy efficiency is as follows [49]:

$$\zeta_{ex} = \frac{\dot{E}x_{el} + \dot{E}x_h + \dot{E}x_c}{\dot{E}x_{con} + \dot{E}x_{solar,in}} \quad (25)$$

where  $\dot{E}x_h$  and  $\dot{E}x_c$  are the heating and cooling exergy, while  $\dot{E}x_{con}$  is the power consumption exergy.

One of the key metrics for determining the system's economic effectiveness is the payback period (PP). For the initial system investment cost  $Z_0$  and system annual net profit  $C_F$ , when  $Z_0$  is the sum of all equipment costs in the system,  $C_F$  is calculated as follows:

$$C_F = Y_{el}E_{el} + Y_hE_h + Y_cE_c - C_{Con} \quad (26)$$

In which  $Y$  (CNY/kWh) is the profit of per unit product,  $E$  (kWh) is the net product generated by the system, the subscripts  $el$ ,  $h$ ,  $c$  represent the electricity, heating and cooling respectively, and  $C_{Con}$  indicates the system energy consumption cost.

Moreover, the payback period  $PP$  is calculated as follows [49]:

$$PP = \frac{Z_0}{C_F} \quad (27)$$

Thus, in order to evaluate the benefit/cost of the unit product energy or exergy, the equipment cost rate  $\dot{Z}_k$  is introduced as follows [50]:

$$\dot{Z}_k = \dot{Z}_k^0 + \dot{Z}_k^{OM} \quad (28)$$

$$\dot{Z}_k^{CI} = \frac{CRC \cdot Z_k}{\tau} \quad (29)$$

$$\dot{Z}_k^{OM} = \frac{\gamma_k \cdot Z_k}{\tau} \quad (30)$$

where  $\dot{Z}_k^0$  is the equipment purchase cost rate and  $\dot{Z}_k^{OM}$  is the operating maintenance cost rate.  $\gamma_k$  and  $\tau$  are the maintenance coefficient and operating hours.  $CRC$  is the capital recovery coefficient, as follows [51]:

$$CRC = \frac{IR(1 + IR)^n}{(1 + IR)^n - 1} \quad (31)$$

where  $IR$  (%) is interest rate,  $n$  is system operation life.

The calculation of the unit product energy profit ( $Y$ ) is defined as [52]:

$$Y = \frac{C_F - \dot{Z}_k \cdot \tau}{E_{el} + E_c + E_h} \quad (32)$$

Moreover, from the perspective of exergy analysis, the unit product exergy cost is also proposed, shown as follows [52]:

$$UPC = \frac{\dot{Z}_k \cdot \tau}{\dot{E}x_{el} + \dot{E}x_c + \dot{E}x_h} \quad (33)$$

Specifically, all relevant economic indicators and parameters are summarized in Table 4, in which the equipment cost, product income and operation cost are determined according to the real-time prices in Tianjin.

**Table 4.** System economic parameters.

Parameter	Value	Unit
Specific cost of equipment	PV/T	680.34
	LHP	266.67
	HHP	500.00
	AC	1065.60
	TES	325.00
Specific profit of production	Space heating	80.00 [53]
	Cooling	0.13
	Power generation	0.37
Other parameters	Specific cost for electricity purchase	0.50 [53]
	Operation and maintenance factor	1.0%
	Interest rate	5.4% [51]
	System operation life	20
		years

#### 4. Validation

In this paper, previous experimental research regarding PV/T, water source heat pump, and absorption chiller are cited, and the meteorological data and equipment parameters set in TRNSYS are the same as those presented in the previous literature. The differences between the simulation data and experimental data are compared to validate the rationality of the models. When the deviation is small, the validity of the model can be proven.

As reported in Ref. [54], the above system model is validated according to the experimental data. Figure 7 displays the comparison results of the PV/T outlet temperature. The simulation result of PV/T model displays good correspondence with the experimental data. The average deviation is 2.91%, which demonstrates good agreement as the deviation is within 10% [38].

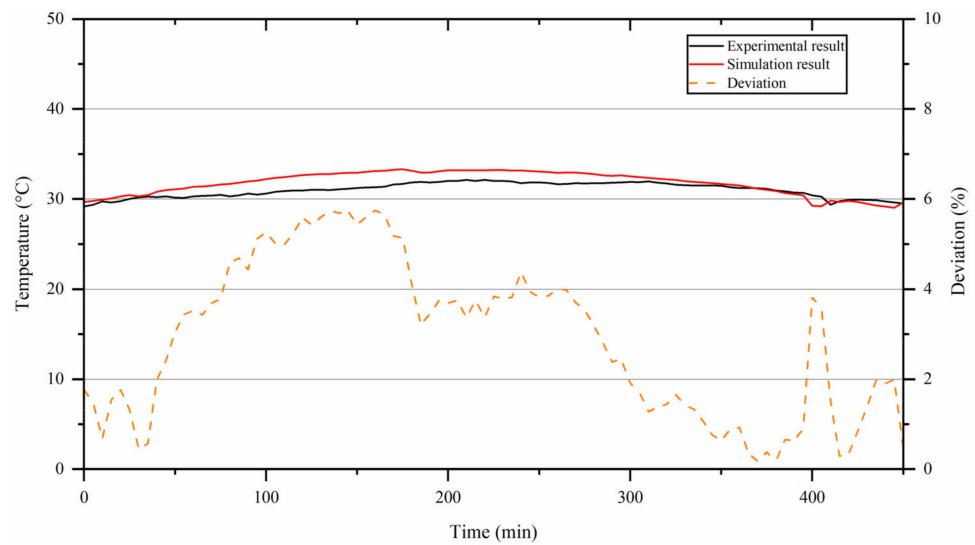


Figure 7. Comparison between experimental and simulation output temperature of PV/T.

Moreover, based on the study investigated by Ref. [55], the experimental data were adopted to validate the HP. Figure 8 indicates the variation in heating capacity under different inlet temperatures of the evaporator. The simulation results closely match with the reference results that the average deviation of the heating capacity is 4.82% and the input power’s average deviation is 5.51%. Therefore, the proposed HP model is validated.

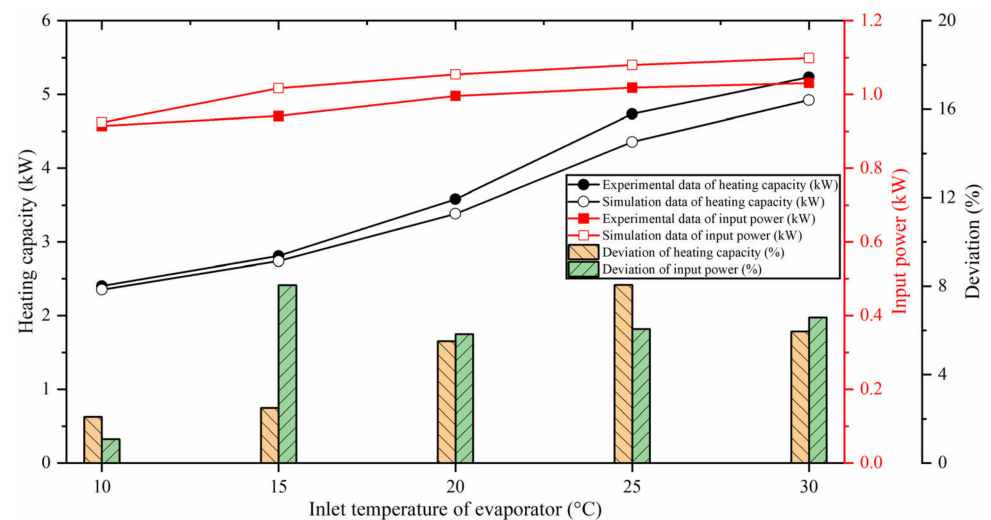


Figure 8. Comparison of simulation and reference results of HP.

Figure 9 displays the cooling capacity of the absorption chiller and the deviation between the simulation and experimental data, according to Ref. [56]. The average deviation between the simulation result and the experimental data is 1.46%.

Finally, it should be pointed out that the effectiveness of the system cannot be validated because of the lack of relevant experimental research, and the components in TRNSYS were the validation of experimental data [57]. Therefore, this paper validates the effectiveness of the system by validating each component.

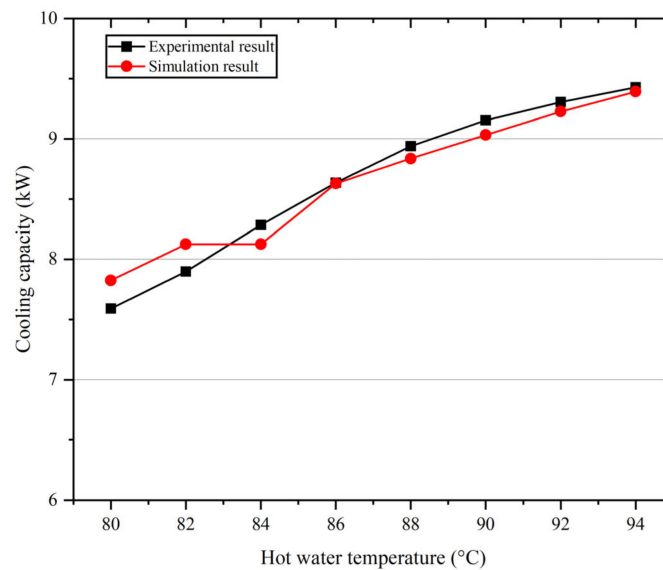


Figure 9. Comparison of simulation and reference results of AC.

## 5. Results and Discussion

Herein, the dynamic research was carried out based on energy, exergy, and economic impact. In addition, parametric evaluations were also made to study the variations in thermodynamic and economic performance with different PV/T areas and LHP capacities.

### 5.1. Energy Analysis

Figure 10 depicts the building load and the energy produced by the solar tri-generation supply system. Approximately 1.23 MWh of auxiliary heat was needed in January, and 0.71 MWh of auxiliary heat was needed in December. The heating and cooling demand was met by the tri-generation system proposed in this paper for other months of the year. In summary, the heating and cooling output generated by system can meet the load requirement, proving the feasibility of the proposed system.

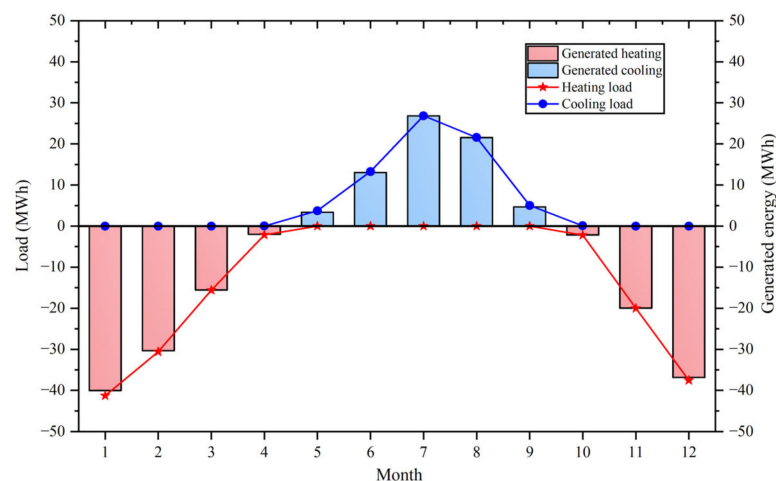


Figure 10. Generated energy and load requirement.

Figure 11 shows the energy performance of equipment throughout the year. The PV/T had an average electrical efficiency of 15.64%, and the wintertime thermal efficiency was 47.40%. In the transitional season (from March to May and from September to October), due to the small cooling and heating loads required, an incomplete utilization of heat output from the PV/T resulted in the increase in the inlet water temperature and a decrease in the thermal efficiency. In the summer, the highest thermal efficiency occurred in August and was equal to 53.42%, with an overall efficiency of 68.89%. Moreover, the COP of the LHP ranged from

2.8 to 3.4, while the COP of the HHP was 1.9 to 2.2. It can be concluded that the evaporator temperature of the LHP was raised accordingly. The COP of the HHP increased slightly with the effect of the PV/T. Moreover, the average COP of the AC was 0.6.

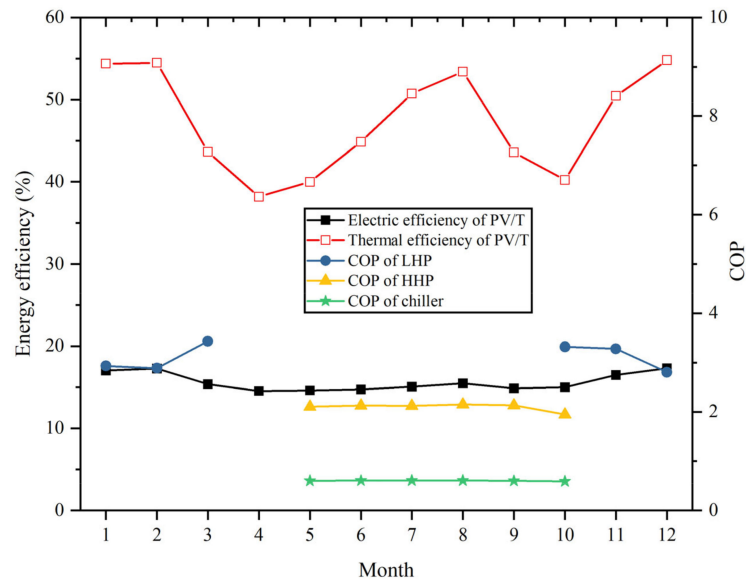


Figure 11. Monthly energy performance of equipment.

Figure 12 depicts the auxiliary equipment power consumption and the PV/T power production. The PV/T generates 171.69 MWh of electricity, while the power consumption is 116.31 MWh. However, in July, August, and December, the power output of the PV/T is lower than the power consumption due to the large energy consumption of the equipment and inappropriate environmental conditions.

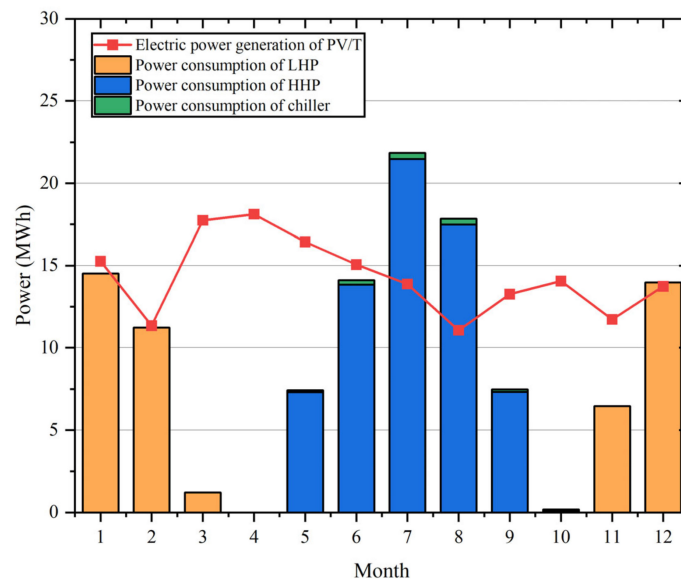


Figure 12. Power production of PV/T and system power consumption.

Figure 13 displays the power consumption coverage by the PV/T in the system. Since no battery is installed, only part of the energy consumption is covered by the PV/T. The PV/T essentially covers the system energy needs during the transitional period, and the PV/T power production provides more than 50% of the energy needed throughout the winter. However, the coverage rate is only 30% due to the large energy consumption in the summer. Nevertheless, the system still maintains a relatively high electricity coverage without using a battery.

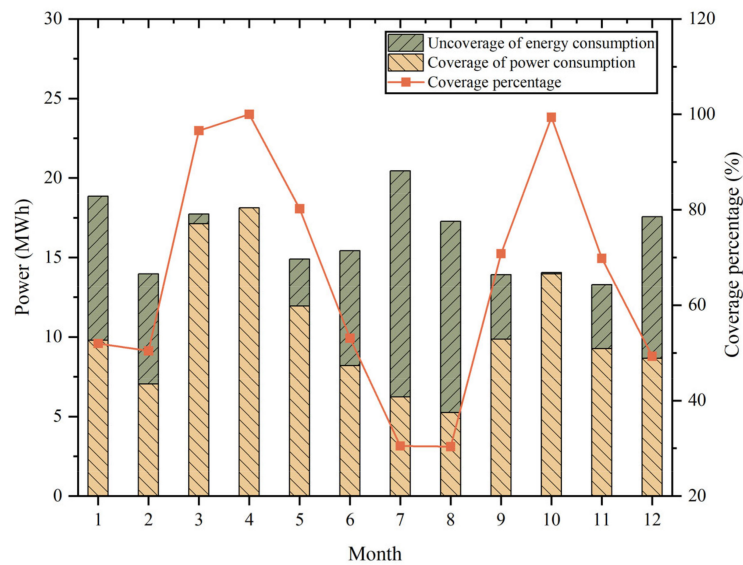


Figure 13. Power consumption coverage by PV/T in the system.

5.2. Exergy Analysis

The electrical and thermal exergy efficiency of the PV/T are shown in Figure 14. The average electrical and thermal efficiency are 16.71% and 1.71%, respectively. It is worth noting that the thermal exergy efficiency shows an opposite trend to the thermal efficiency in Figure 11, which is related to the temperature of the hot water in the PV/T. While increasing the hot water temperature improves the thermal exergy efficiency, it also increases the heat transfer resistance between the PV cell and the cooling water, leading to a decrease in the PV/T thermal efficiency. In addition, the average exergy efficiency of the LHP is 36.17%. The average exergy efficiency of the HHP is 22.54%, while the exergy efficiency of the AC is 19.29%.

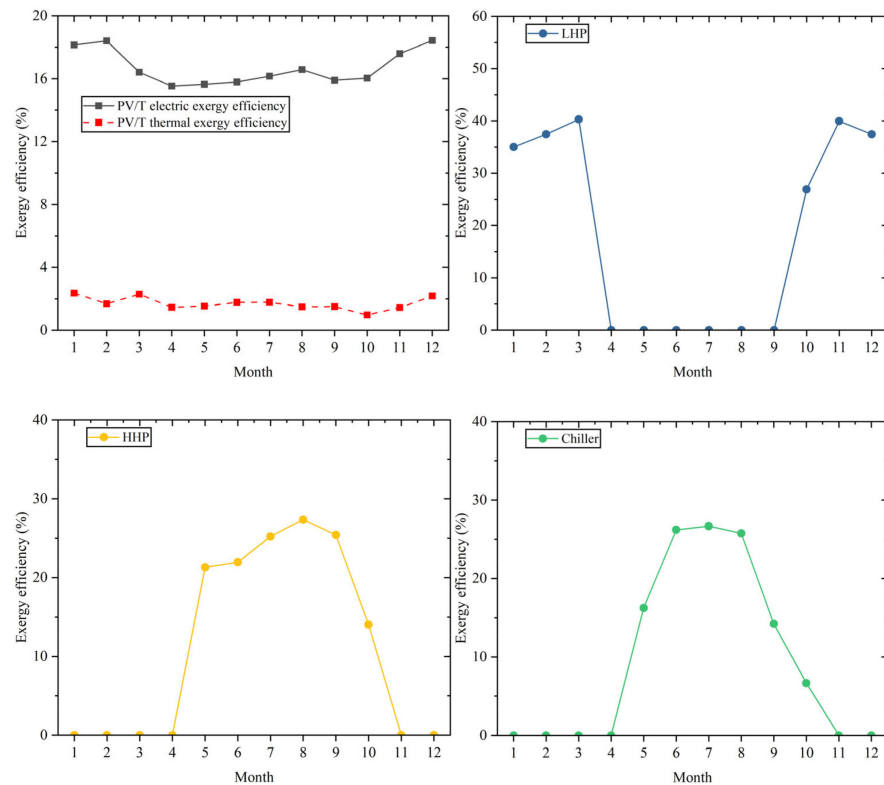


Figure 14. Exergy efficiency of each equipment.

Figure 15 displays the exergy flow stream of the system throughout the year. Only a small portion of solar exergy is converted into electrical and thermal exergy by the PV/T, while the rest is the exergy destruction. Additionally, the electrical exergy generated by the PV/T is much higher than thermal exergy due to the difference in energy quality. Similarly, compared to the energy consumption, the thermal exergy of the PV/T only accounts for a small proportion of the input to the low-temperature heat pump and the high-temperature heat pump. It is worth noting that the high-temperature heat pump has the highest exergy destruction besides the solar exergy destruction, which is also reflected in Figure 16. The auxiliary equipment exergy destruction accounts for only 9.9% of the total exergy destruction, while the high-temperature heat pump is 54.5% of the auxiliary equipment exergy destruction because of the higher temperature difference between the hot and cold sides of the high-temperature heat pump and the higher power consumption.

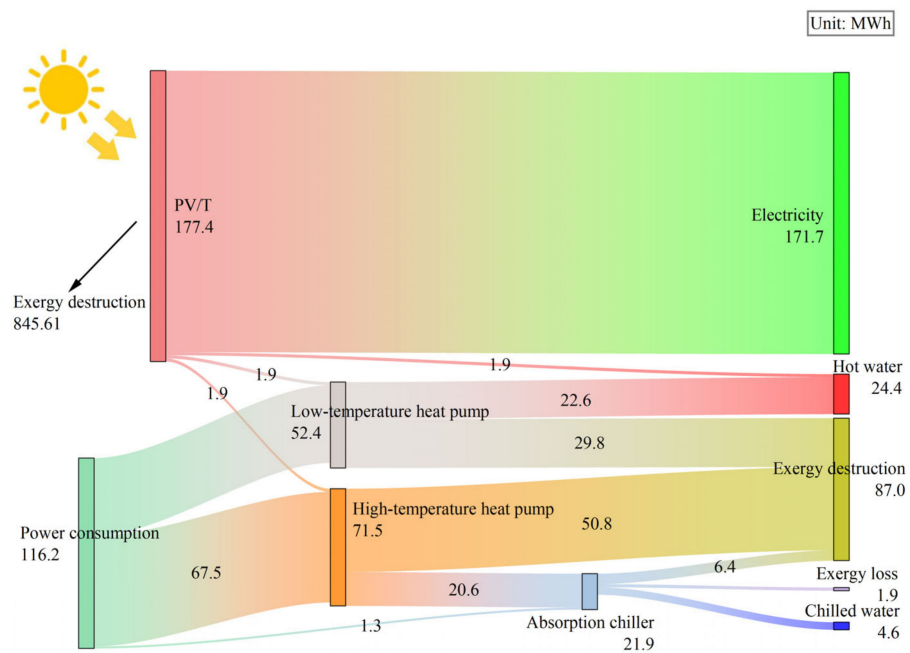


Figure 15. Exergy flow stream process of system.

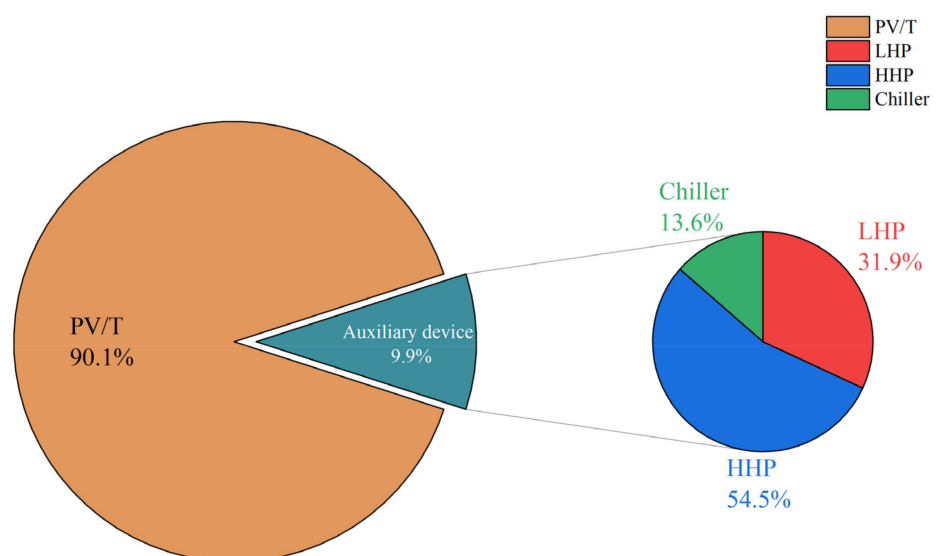


Figure 16. Proportion of exergy destruction of equipment.

Figure 17 illustrates the monthly energy and exergy efficiency of the system. The average energy efficiency is 32.98%, while the average exergy efficiency is 17.62%. The energy efficiency and exergy efficiency of the system is higher in winter due to the higher heating demand and lower energy consumption, as well as the smaller exergy destruction of the low-temperature heat pump in the winter.

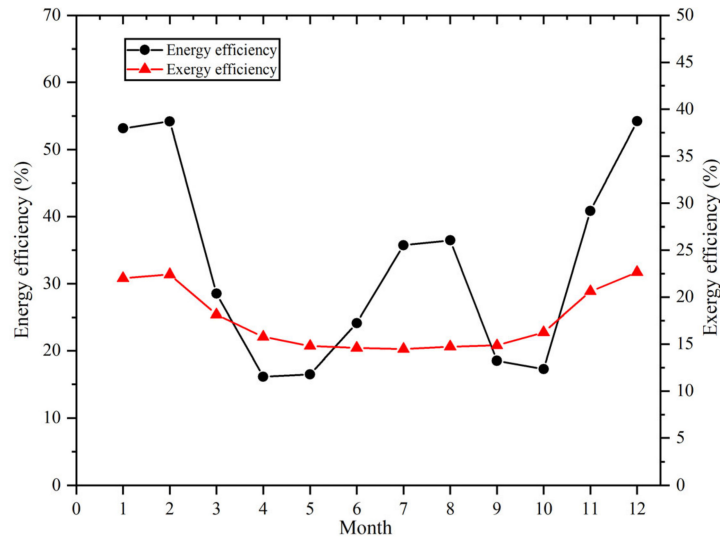


Figure 17. Monthly energy and exergy efficiency of system.

5.3. Economic Analysis

The monthly profit and cost of the system is investigated in Figure 18. Generally, the annual profit includes heating, electricity, and cooling. The heating profit is higher in winter than the electricity profit during the transitional season, and the cooling profit is the lowest in summer, even close to zero. As a result, the overall annual profit represents a high value in the winter and a low value in the summer. During the heating season, the profit mainly comes from space heating. As the system energy consumption decreases during the transition season, the net electricity profit becomes the majority. In the summer, due to the high energy consumption of the HHP, an operation cost of about 2481.09 CNY is required for an electricity purchase from the grid in July. Table 5 lists the economic results of the system. The payback period is 7.77 years, the unit product energy profit is 0.050 CNY/kWh, and the unit product exergy cost is 0.120 CNY/kWh.

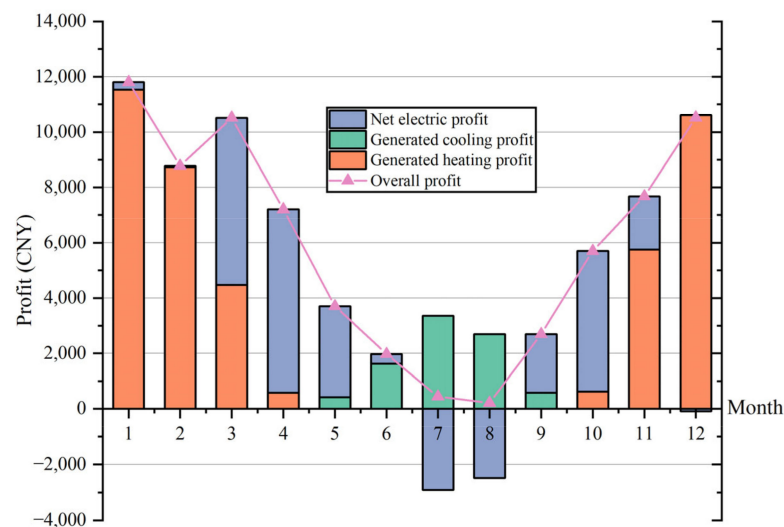


Figure 18. Monthly economic profit and cost of system.

**Table 5.** The main system economic analysis factor.

PP (Years)	Cost Rate of the System (CNY/h)	Unit Product Energy Profit (CNY/kWh)	Unit Product Exergy Cost (CNY/kWh)
7.77	5.32	0.050	0.120

#### 5.4. Comparisons with Relevant Research

In addition, Table 6 shows the comparison between evaluation indicators of the present study with other relevant research studies. The proposed system demonstrates an improvement over the previous research, with advantages in energy efficiency, exergy efficiency, and the payback period.

**Table 6.** Performance indicator comparison between the present study and relevant research.

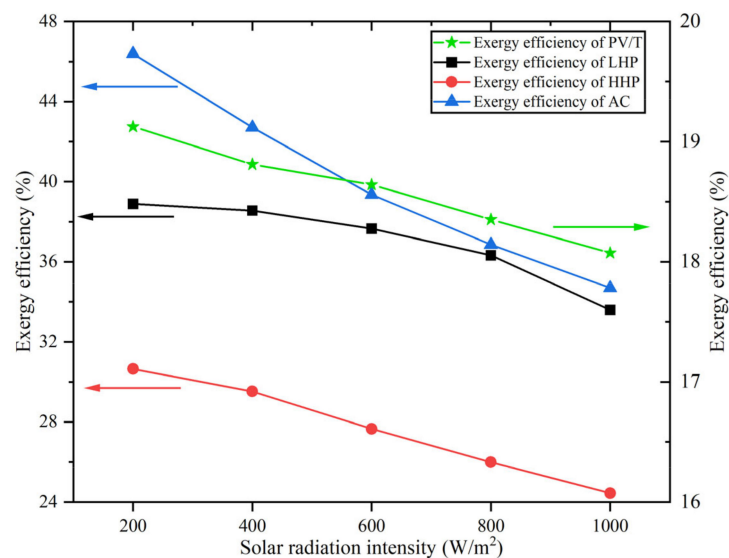
System	Energy Efficiency	Exergy Efficiency	PP (Years)
Present study	31.72%	17.35%	7.77
Ural et al. [58]	-	14.40%	-
Obalanlege et al. [59]	-	-	14
Chen et al. [60]	29.60%	-	-

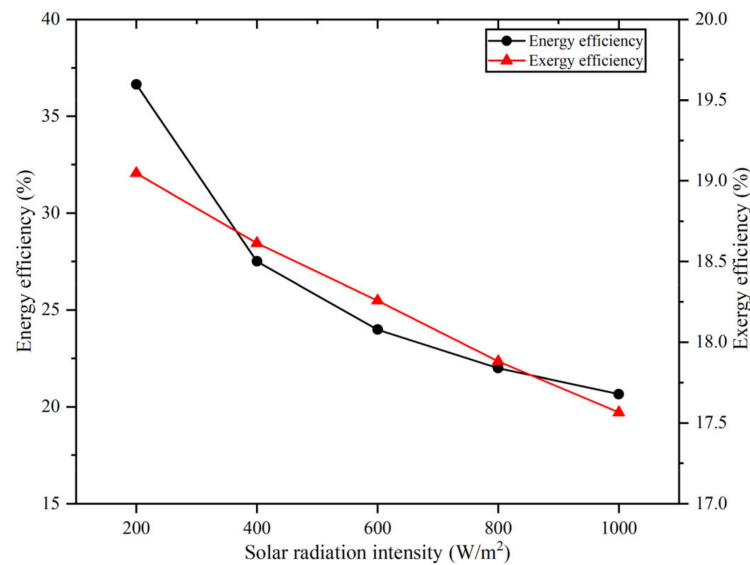
#### 5.5. Parametric Analysis

In this paper, the parametric analysis was performed. The solar radiation intensity, PV/T area, and LHP capacity were selected as key parameters to study the influence of changing the key parameters on the system energy efficiency, exergy efficiency, and economic indicators.

##### (1) Effect of solar radiation intensity

Firstly, it can be observed from Figures 19 and 20 that when the solar radiation intensity increases, a decreasing trend can be seen in the exergy efficiency of both the equipment and the system. This is an acceptable result because the increased solar radiation intensity leads to an increase in the amount of input energy, while the increase in the energy output is relatively small.

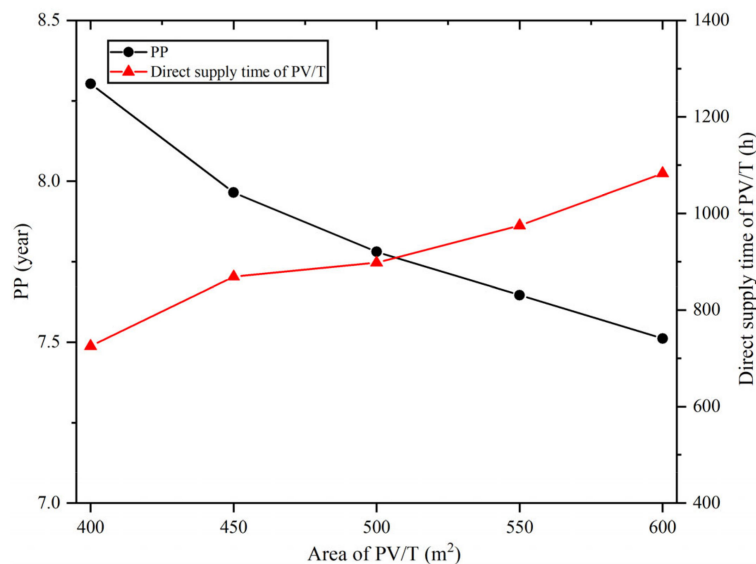
**Figure 19.** Exergy efficiency of equipment with different solar radiation intensity.



**Figure 20.** System exergy efficiency with different solar radiation intensity.

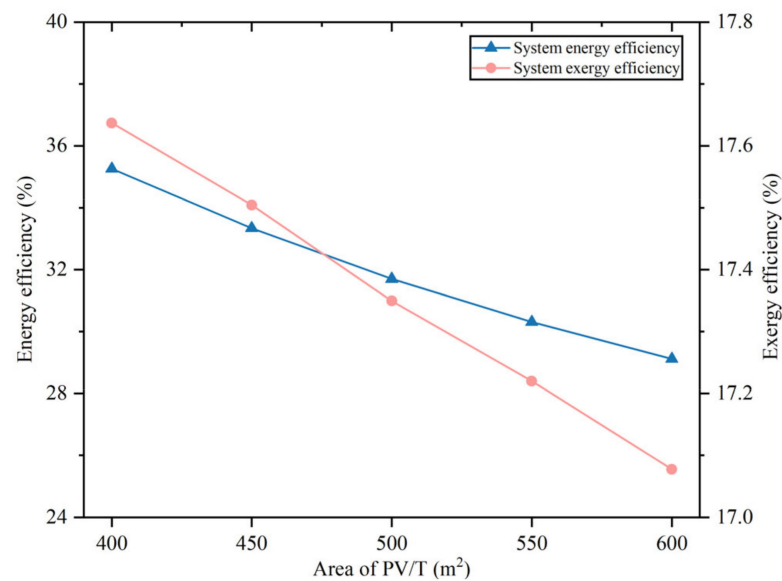
## (2) Effect of variable PV/T area

Figure 21 indicates a variation between the PP and the direct supply time with different PV/T areas. With an increase in the PV/T area, the direct supply time of the PV/T keeps increasing since more hot water from the TES meets the space heating requirement. Moreover, with an increase in the PV/T direct supply time, the LHP operation time correspondingly decreases; that is, the system power consumption is also reduced. The increase in the net profit still effectively reduces the PP, even if it leads to an increase in the initial investment cost with the increase in the PV/T area.



**Figure 21.** Variation between PP and direct supply time with different area of PV/T.

Figure 22 shows the variation between system energy and exergy efficiency with different areas of the PV/T. The system efficiency decreases because the solar radiation intensity input rises, while changes in the cooling and heating loads and power generation are relatively small. Furthermore, the system efficiency decreases from 17.64% to 17.08% with the increase in solar exergy input.



**Figure 22.** Variation between system energy efficiency and exergy efficiency with different area of PV/T.

In general, the proportion of solar energy in the product and the economic performance are generally improved by increasing the PV/T area, even if it results in decreased system efficiency. In general, increasing the PV/T area is advantage to the system. However, as the PV/T area is limited by the actual installable area of the building roof, it is significant to arrange the layout such that the PV/T area is increased as much as possible.

### (3) Influence of variable LHP capacity

Figure 23 shows the variation between the PP and the direct supply time with different LHP capacities. The total energy consumption increases and reaches a maximum value as the capacity increases from 52 kW to 68 kW. Moreover, with the capacity increase, the system satisfied heating load increases until a maximum value. Continuing to increase the capacity would decrease the LHP operating time, resulting in a decrease in energy consumption. The change in the PP is small, from 52 kW to 68 kW, and the PP decreases rapidly when the capacity increases from 68 kW to 92 kW. The increase in the heating load leads to an increase in the heating profit, which is neutralized by the increase in energy consumption cost and initial investment cost, resulting in a small change in the PP. However, as the capacity continues to increase, the energy consumption decreases, resulting in an evident decrease in the PP. The direct supply time of the PV/T increases because the increased capacity causes the temperature of the hot water flowing into the building to rise, which in turn raises the TES temperature. Figure 24 illustrates the changes in system energy efficiency and exergy efficiency with different LHP capacities. Both energy efficiency and exergy efficiency improve as the capacity increases. The increase from 52 kW to 68 kW is mainly due to the increase in the heating load, while the increase from 68 kW to 92 kW is mainly due to the decrease in the power consumption, which is the primary factor affecting the system efficiency.

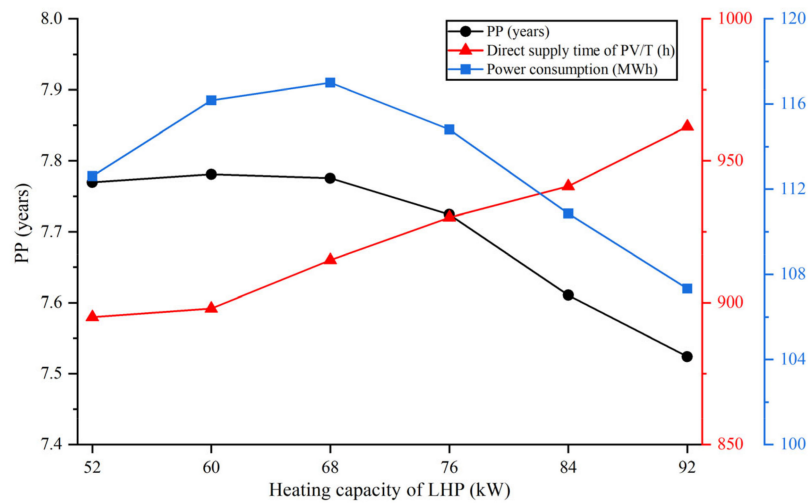


**Figure 23.** Variation between PP and direct supply time with different capacities of LHP.

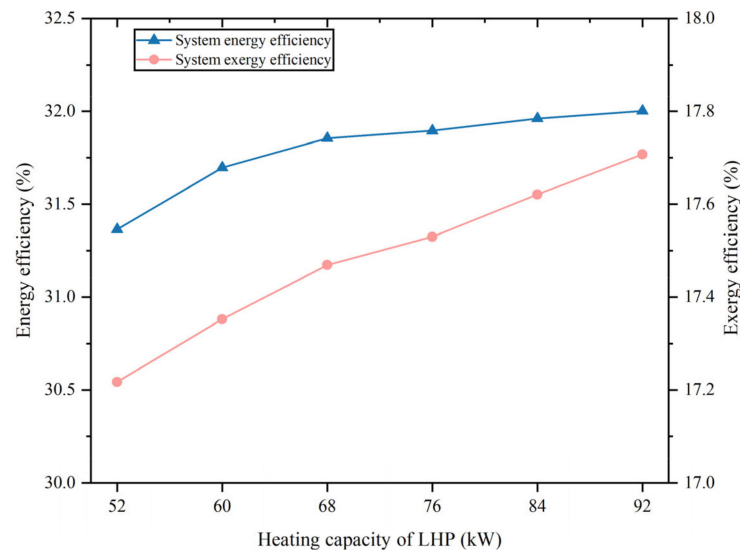


**Figure 24.** Variation between system energy and exergy efficiency with different capacities of LHP.

## 6. Conclusions

To overcome the impact of solar energy randomness on building energy supply and to solve the issue of temperature mismatch and heating instability in a PV/T-AC system, a distributed solar energy system suitable for an urban building was proposed. In this study, a system model was established using TRNSYS, which adopted a PV/T and a water-source heat pump to provide stable heating for the building and absorption chiller. The system was examined from energy, exergy, and economic analysis perspectives, and a parametric analysis was conducted. The conclusions are as follows:

- (1) The system can satisfy the building load, which is crucial for verifying the feasibility of the proposed system.
- (2) In terms of system performance evaluation, the layout based on a PV/T, a heat pump, and an absorption chiller achieves an average energy efficiency of 32.98% and an average exergy efficiency of 17.62%. Additionally, the payback period of the proposed system is 7.77 years. Compared to the systems in the other literature, the proposed system in this paper has certain performance advantages.
- (3) Increasing the area of the PV/T shortened the payback period of the system, which has a positive impact on the tri-generation system. However, the PV/T area is restricted to the actual area of the building roof; thus, the layout of the PV/T should be reasonably arranged to achieve a maximum installed area. Furthermore, increasing

the LHP capacity brings an increase in the energy efficiency and exergy efficiency and a decrease in the payback period.

This study aims to provide quantitative performance data to support the promotion of a distributed solar energy system in an urban area. It provides a new solution for achieving a near-zero-emission building. In future research, an experimental platform based on this layout will be built to evaluate its performance operation in an actual environment.

**Author Contributions:** Conceptualization, H.Y., Z.X. and D.A.; methodology, H.Y.; software, S.C.; validation, Z.X. and C.C.; formal analysis, H.Y. and S.C.; investigation, C.C. and H.Z.; resources, H.Z.; data curation, H.Y. and C.C.; writing—original draft preparation, Z.X.; writing—review and editing, H.C.; visualization, H.Y.; supervision, S.C.; project administration, H.Z.; funding acquisition, H.Z. All authors have read and agreed to the published version of the manuscript.

**Funding:** This research was funded by the National Natural Science Foundation of China (CN), 52006063.

**Data Availability Statement:** The data used to support the findings of this study are available from the corresponding author upon request.

**Conflicts of Interest:** The authors declare no conflict of interest.

### Abbreviations

CNY	Chinese yuan
COP	Coefficient of performance
CRC	Capital recovery factor
CT	Cooling tower
HP	Heat pump
HX	Heat exchanger
OM	Operation and maintenance
PV/T	Photovoltaic/thermal
TES	Thermal energy storage

### Symbols

$A_{pv}$	Area of photovoltaic panel ( $m^2$ )
$C_F$	Annual net profit of system (CNY)
$C_{Con}$	Annual energy consumption cost (CNY)
$c_p$	Specific heat capacity ( $J/kg \cdot K$ )
$E$	Annual overall net product (kWh)
$\dot{E}_n$	Energy rate (W)
$\dot{E}_x$	Exergy rate (W)
$G$	Received solar radiation intensity, ( $W/m^2$ )
$IR$	Interest rate (%)
$\dot{m}$	Mass flow rate ( $kg/s$ )
$n$	System life (years)
$P$	Electric power (W)
$PP$	Payback period (years)
$\dot{Q}$	Thermal capacity (W)
$T$	Temperature (K)
$UPC$	Unit product exergy cost (CNY/kWh)
$\dot{W}$	Power consumption (W)
$Y$	Unit product energy profit (CNY/kWh)
$\dot{Z}$	Equipment cost rate (CNY/h)
$Z_0$	Overall initial investment cost of system (CNY)
$Z_k$	Investment cost of each component (CNY)

**Greek Letters**

$\gamma_k$	Maintenance factor
$\xi$	Exergy efficiency (%)
$\eta$	Energy efficiency (%)
$\tau$	Operating hour (h)
$\tau_g$	Transmittance of the glass cover plate
$\psi_s$	Conversion coefficient of solar radiation exergy

**Subscripts**

0	Dead state
<i>a</i>	Ambient
<i>c</i>	Cooling
<i>C</i>	Condenser
<i>con</i>	Consumption
<i>d</i>	Destruction
<i>E</i>	Evaporator
<i>el</i>	Electrical
<i>f</i>	Fuel
<i>G</i>	Generator
<i>h</i>	Heating
<i>in</i>	Inlet
<i>k</i>	<i>k</i> th component
<i>l</i>	Loss
<i>out</i>	Outlet
<i>p</i>	Product
<i>sys</i>	System
<i>th</i>	Thermal

**References**

- IEA. Tracking Buildings, Paris. 2021. Available online: <https://www.iea.org/reports/tracking-buildings-2021> (accessed on 5 August 2022).
- Lin, Y.; Zhong, S.; Yang, W.; Hao, X.; Li, C.-Q. Towards zero-energy buildings in China: A systematic literature review. *J. Clean. Prod.* **2020**, *276*, 123297. [[CrossRef](#)]
- Miglioli, A.; Aste, N.; Del Pero, C.; Leonforte, F. Photovoltaic-thermal solar-assisted heat pump systems for building applications: Integration and design methods. *Energy Built Environ.* **2023**, *4*, 39–56. [[CrossRef](#)]
- Zhao, Y.; Ding, C.; Zhu, J.; Qin, W.; Tao, X.; Fan, F.; Li, R.; Li, C. A Hydrogen Farm Strategy for Scalable Solar Hydrogen Production with Particulate Photocatalysts. *Angew. Chem. Int. Ed.* **2020**, *59*, 9653–9658. [[CrossRef](#)] [[PubMed](#)]
- Eslami, M.; Akbari, E.; Seyed Sadr, S.T.; Ibrahim, B.F. A novel hybrid algorithm based on rat swarm optimization and pattern search for parameter extraction of solar photovoltaic models. *Energy Sci. Eng.* **2022**, *10*, 2689–2713. [[CrossRef](#)]
- Yaghoubi, M.; Eslami, M.; Noroozi, M.; Mohammadi, H.; Kamari, O.; Palani, S. Modified Salp Swarm Optimization for Parameter Estimation of Solar PV Models. *IEEE Access* **2022**, *10*, 110181–110194. [[CrossRef](#)]
- Fraunhofer Institute for Solar Energy Systems. Photovoltaic Report, Technical Report, Freiburg. 2020. Available online: <https://www.ise.fraunhofer.de/content/dam/ise/de/documents/publications/studies/Photovoltaics-Report.pdf> (accessed on 5 August 2022).
- Hasan Ghodusinejad, M.; Ghodrati, A.; Zahedi, R.; Yousefi, H. Multi-criteria modeling and assessment of PV system performance in different climate areas of Iran. *Sustain. Energy Technol. Assess.* **2022**, *53*, 102520. [[CrossRef](#)]
- Arslan, E.; Faruk Can, Ö.; Koşan, M.; Demirtaş, M.; Aktekel, B.; Aktaş, M. Numerical and experimental assessment of a photovoltaic thermal collector using variable air volume. *Therm. Sci. Eng. Prog.* **2023**, *39*, 101735. [[CrossRef](#)]
- Bandaru, S.H.; Becerra, V.; Khanna, S.; Radulovic, J.; Hutchinson, D.; Khusainov, R. A Review of Photovoltaic Thermal (PVT) Technology for Residential Applications: Performance Indicators, Progress, and Opportunities. *Energies* **2021**, *14*, 3853. [[CrossRef](#)]
- Sredensšek, K.; Seme, S.; Štumberger, B.; Hadžiselimović, M.; Chowdhury, A.; Praunseis, Z. Experimental Validation of a Dynamic Photovoltaic/Thermal Collector Model in Combination with a Thermal Energy Storage Tank. *Energies* **2021**, *14*, 8162. [[CrossRef](#)]
- Ochs, F.; Magni, M.; Dermentzis, G. Integration of Heat Pumps in Buildings and District Heating Systems—Evaluation on a Building and Energy System Level. *Energies* **2022**, *15*, 3889. [[CrossRef](#)]
- Jang, Y.; Lee, D.; Kim, J.; Ham, S.H.; Kim, Y. Performance characteristics of a waste-heat recovery water-source heat pump system designed for data centers and residential area in the heating dominated region. *J. Build. Eng.* **2022**, *62*, 105416. [[CrossRef](#)]
- Zhang, T.; Wang, F.; Gao, Y.; Liu, Y.; Guo, Q.; Zhao, Q. Optimization of a solar-air source heat pump system in the high-cold and high-altitude area of China. *Energy* **2023**, *268*, 126653. [[CrossRef](#)]
- Besagni, G.; Croci, L.; Nesa, R.; Molinaroli, L. Field study of a novel solar-assisted dual-source multifunctional heat pump. *Renew. Energy* **2019**, *132*, 1185–1215. [[CrossRef](#)]

16. Zhou, J.; Zhao, X.; Ma, X.; Qiu, Z.; Ji, J.; Du, Z.; Yu, M. Experimental investigation of a solar driven direct-expansion heat pump system employing the novel PV/micro-channels-evaporator modules. *Appl. Energy* **2016**, *178*, 484–495. [[CrossRef](#)]
17. Ren, H.; Sun, Y.; Albdoor, A.K.; Tyagi, V.V.; Pandey, A.K.; Ma, Z. Improving energy flexibility of a net-zero energy house using a solar-assisted air conditioning system with thermal energy storage and demand-side management. *Appl. Energy* **2021**, *285*, 116433. [[CrossRef](#)]
18. Aneli, S.; Gagliano, A.; Tina, G.M.; Gediz Ilis, G.; Demir, H. Effectiveness and constraints of using PV/Thermal collectors for heat-driven chillers. *Appl. Therm. Eng.* **2022**, *210*, 118330. [[CrossRef](#)]
19. Liu, M.; Cheng, Y.; Cheng, W.; Zhan, C. Dynamic performance analysis of a solar driving absorption chiller integrated with absorption thermal energy storage. *Energy Convers. Manag.* **2021**, *247*, 114769. [[CrossRef](#)]
20. Karami, M.; Jalalizadeh, M. Performance comparison and risk assessment of BIPVT-based trigeneration systems using vapor compression and absorption chillers. *J. Build. Eng.* **2023**, *69*, 106244. [[CrossRef](#)]
21. Kazem, H.A. Evaluation and analysis of water-based photovoltaic/thermal (PV/T) system. *Case Stud. Therm. Eng.* **2019**, *13*, 100401. [[CrossRef](#)]
22. Abdul-Ganiyu, S.; Quansah, D.A.; Ramde, E.W.; Seidu, R.; Adaramola, M.S. Study effect of flow rate on flat-plate water-based photovoltaic-thermal (PVT) system performance by analytical technique. *J. Clean. Prod.* **2021**, *321*, 128985. [[CrossRef](#)]
23. Odeh, S.; Feng, J. Long Term Performance Assessment of a Residential PV/Thermal Hybrid System. *Energies* **2022**, *16*, 121. [[CrossRef](#)]
24. Maoulida, F.; Djedjig, R.; Kassim, M.A.; El Ganaoui, M. Numerical Study for the Evaluation of the Effectiveness and Benefits of Using Photovoltaic-Thermal (PV/T) System for Hot Water and Electricity Production under a Tropical African Climate: Case of Comoros. *Energies* **2022**, *16*, 240. [[CrossRef](#)]
25. Hassan, A.; Abbas, S.; Yousuf, S.; Abbas, F.; Amin, N.M.; Ali, S.; Shahid Mastoi, M. An experimental and numerical study on the impact of various parameters in improving the heat transfer performance characteristics of a water based photovoltaic thermal system. *Renew. Energy* **2023**, *202*, 499–512. [[CrossRef](#)]
26. Kalateh, M.R.; Kianifar, A.; Sardarabadi, M. Energy, exergy, and entropy generation analyses of a water-based photovoltaic thermal system, equipped with clockwise counter-clockwise twisted tapes: An indoor experimental study. *Appl. Therm. Eng.* **2022**, *215*, 118906. [[CrossRef](#)]
27. Parthiban, A.; Reddy, K.S.; Pesala, B.; Mallick, T.K. Effects of operational and environmental parameters on the performance of a solar photovoltaic-thermal collector. *Energy Convers. Manag.* **2020**, *205*, 112428. [[CrossRef](#)]
28. Gao, D.; Zhao, Y.; Liang, K.; He, S.; Zhang, H.; Chen, H. Energy and exergy analyses of a low-concentration photovoltaic/thermal module with glass channel. *Energy* **2022**, *253*, 124058. [[CrossRef](#)]
29. Liu, W.; Yao, J.; Jia, T.; Zhao, Y.; Dai, Y.; Zhu, J.; Novakovic, V. The performance optimization of DX-PVT heat pump system for residential heating. *Renew. Energy* **2023**, *206*, 1106–1119. [[CrossRef](#)]
30. Sanz, A.; Martín, A.J.; Pereda, A.; Román, E.; Ibañez, P.; Fuente, R. A Solar Dually PVT Driven Direct Expansion Heat Pump One-Year Field Operation Results at Continental Climate. *Energies* **2022**, *15*, 3205. [[CrossRef](#)]
31. Pakere, I.; Blumberga, D. Solar power or solar heat: What will upraise the efficiency of district heating? Multi-criteria analyses approach. *Energy* **2020**, *198*, 117291. [[CrossRef](#)]
32. Koşan, M.; Aktaş, M. Performance investigation of a double pass PVT assisted heat pump system with latent heat storage unit. *Appl. Therm. Eng.* **2021**, *199*, 117524. [[CrossRef](#)]
33. Mi, P.; Zhang, J.; Han, Y.; Guo, X. Study on energy efficiency and economic performance of district heating system of energy saving reconstruction with photovoltaic thermal heat pump. *Energy Convers. Manag.* **2021**, *247*, 114677. [[CrossRef](#)]
34. Bae, S.; Chae, S.; Nam, Y. Performance Analysis of Integrated Photovoltaic-Thermal and Air Source Heat Pump System through Energy Simulation. *Energies* **2022**, *15*, 528. [[CrossRef](#)]
35. Yao, J.; Dou, P.; Zheng, S.; Zhao, Y.; Dai, Y.; Zhu, J.; Novakovic, V. Co-generation ability investigation of the novel structured PVT heat pump system and its effect on the “Carbon neutral” strategy of Shanghai. *Energy* **2022**, *239*, 121863. [[CrossRef](#)]
36. Rijvers, L.; Rindt, C.; de Keizer, C. Numerical Analysis of a Residential Energy System That Integrates Hybrid Solar Modules (PVT) with a Heat Pump. *Energies* **2021**, *15*, 96. [[CrossRef](#)]
37. Kong, R.; Deethayat, T.; Asanakham, A.; Kiatsiroat, T. Performance and economic evaluation of a photovoltaic/thermal (PV/T)-cascade heat pump for combined cooling, heat and power in tropical climate area. *J. Energy Storage* **2020**, *30*, 101507. [[CrossRef](#)]
38. Li, Z.; Chen, H.; Xu, Y.; Tiow Ooi, K. Comprehensive evaluation of low-grade solar trigeneration system by photovoltaic-thermal collectors. *Energy Convers. Manag.* **2020**, *215*, 112895. [[CrossRef](#)]
39. Chen, H.; Li, Z.; Xu, Y. Evaluation and comparison of solar trigeneration systems based on photovoltaic thermal collectors for subtropical climates. *Energy Convers. Manag.* **2019**, *199*, 111959. [[CrossRef](#)]
40. Gholamian, E.; Hanafizadeh, P.; Ahmadi, P.; Mazzarella, L. A transient optimization and techno-economic assessment of a building integrated combined cooling, heating and power system in Tehran. *Energy Convers. Manag.* **2020**, *217*, 112962. [[CrossRef](#)]
41. Cao, Y.; Dhahad, H.A.; Hussien, H.M.; Parikhani, T. Proposal and evaluation of two innovative combined gas turbine and ejector refrigeration cycles fueled by biogas: Thermodynamic and optimization analysis. *Renew. Energy* **2022**, *181*, 749–764. [[CrossRef](#)]
42. Kai, L.; Heng, Z.; Haiping, C.; Jiguang, H.; Xinxin, G. The comparison study between different battery and channel of the LCPV/T systems under concentration ratio 4. *Energy* **2020**, *191*, 116492. [[CrossRef](#)]

43. Zheng, N.; Zhang, H.; Duan, L.; Wang, X.; Liu, L. Energy, exergy, exergoeconomic and exergoenvironmental analysis and optimization of a novel partially covered parabolic trough photovoltaic thermal collector based on life cycle method. *Renew. Energy* **2022**, *200*, 1573–1588. [[CrossRef](#)]
44. Liu, Y.; Zhang, H.; Chen, H. Experimental study of an indirect-expansion heat pump system based on solar low-concentrating photovoltaic/thermal collectors. *Renew. Energy* **2020**, *157*, 718–730. [[CrossRef](#)]
45. Yang, L.; Heng, Z.; Haiping, C.; Han, Y.; Fei, Y. Simulating and experimental research on a low-concentrating PV/T triple-generation system. *Energy Convers. Manag.* **2019**, *199*, 111942. [[CrossRef](#)]
46. Zhang, H.; Pan, X.; Chen, J.; Xie, J. Energy, exergy, economic and environmental analyses of a cascade absorption-compression refrigeration system using two-stage compression with complete intercooling. *Appl. Therm. Eng.* **2023**, *225*, 120185. [[CrossRef](#)]
47. Buonomano, A.; Calise, F.; Palombo, A.; Vicidomini, M. Transient analysis, exergy and thermo-economic modelling of façade integrated photovoltaic/thermal solar collectors. *Renew. Energy* **2019**, *137*, 109–126. [[CrossRef](#)]
48. Wang, J.; Lu, Z.; Li, M.; Lior, N.; Li, W. Energy, exergy, exergoeconomic and environmental (4E) analysis of a distributed generation solar-assisted CCHP (combined cooling, heating and power) gas turbine system. *Energy* **2019**, *175*, 1246–1258. [[CrossRef](#)]
49. Zarei, A.; Akhavan, S.; Rabiee, M.B.; Elahi, S. Energy, exergy and economic analysis of a novel solar driven CCHP system powered by organic Rankine cycle and photovoltaic thermal collector. *Appl. Therm. Eng.* **2021**, *194*, 117091. [[CrossRef](#)]
50. Vojdani, M.; Fakhari, I.; Ahmadi, P. A novel triple pressure HRSG integrated with MED/SOFC/GT for cogeneration of electricity and freshwater: Techno-economic-environmental assessment, and multi-objective optimization. *Energy Convers. Manag.* **2021**, *233*, 113876. [[CrossRef](#)]
51. Song, Y.; Mu, H.; Li, N.; Shi, X.; Zhao, X.; Chen, C.; Wang, H. Techno-economic analysis of a hybrid energy system for CCHP and hydrogen production based on solar energy. *Int. J. Hydrog. Energy* **2022**, *47*, 24533–24547. [[CrossRef](#)]
52. Colakoglu, M.; Durmayaz, A. Energy, exergy, economic and emission saving analysis and multiobjective optimization of a new multi-generation system based on a solar tower with triple combined power cycle. *Sustain. Energy Technol. Assess.* **2022**, *52*, 102289. [[CrossRef](#)]
53. Ma, H.; Li, C.; Lu, W.; Zhang, Z.; Yu, S.; Du, N. Experimental study of a multi-energy complementary heating system based on a solar-groundwater heat pump unit. *Appl. Therm. Eng.* **2016**, *109*, 718–726. [[CrossRef](#)]
54. Sakellariou, E.; Axaopoulos, P. An experimentally validated, transient model for sheet and tube PVT collector. *Sol. Energy* **2018**, *174*, 709–718. [[CrossRef](#)]
55. Qu, M.; Chen, J.; Nie, L.; Li, F.; Yu, Q.; Wang, T. Experimental study on the operating characteristics of a novel photovoltaic/thermal integrated dual-source heat pump water heating system. *Appl. Therm. Eng.* **2016**, *94*, 819–826. [[CrossRef](#)]
56. Heng, Z.; Feipeng, C.; Yang, L.; Haiping, C.; Kai, L.; Boran, Y. The performance analysis of a LCPV/T assisted absorption refrigeration system. *Renew. Energy* **2019**, *143*, 1852–1864. [[CrossRef](#)]
57. Calise, F.; d’Accadia, M.D.; Vicidomini, M. Optimization and dynamic analysis of a novel polygeneration system producing heat, cool and fresh water. *Renew. Energy* **2019**, *143*, 1331–1347. [[CrossRef](#)]
58. Ural, T.; Karaca Dolgun, G.; Güler, O.V.; Keçebaş, A. Performance analysis of a textile based solar assisted air source heat pump with the energy and exergy methodology. *Sustain. Energy Technol. Assess.* **2021**, *47*, 101534. [[CrossRef](#)]
59. Obalanlege, M.A.; Xu, J.; Markides, C.N.; Mahmoudi, Y. Techno-economic analysis of a hybrid photovoltaic-thermal solar-assisted heat pump system for domestic hot water and power generation. *Renew. Energy* **2022**, *196*, 720–736. [[CrossRef](#)]
60. Chen, J.; Zhang, Z.; Zhang, G.; Wang, D. Energy, exergy, economic and environmental analysis of a novel direct-expansion solar-assisted flash tank vapor injection heat pump for water heater. *Energy Convers. Manag.* **2022**, *254*, 115239. [[CrossRef](#)]

**Disclaimer/Publisher’s Note:** The statements, opinions and data contained in all publications are solely those of the individual author(s) and contributor(s) and not of MDPI and/or the editor(s). MDPI and/or the editor(s) disclaim responsibility for any injury to people or property resulting from any ideas, methods, instructions or products referred to in the content.